J Radioanal Nucl Chem (2015) 303:237–244
DOI 10.1007/s10967-014-3320-x

Biodistribution of ^{99m}Tc–2-aminoestrone-3-methyl ether as a potential radiotracer for inflammation imaging

Maha S. Al Mutairi · Mohammed A. Motaleb · Nadia G. Haress · Wafaa A. Zaghary

Received: 9 April 2014 / Published online: 19 July 2014

Abstract Estrogens may have pro- and anti-inflammatory properties depending on the situation and the involved tissue. 2-Aminoestrone-3-methyl ether as an estrogenic derivative was prepared with a yield of 55 % and well characterized. ^{99m}Tc–2-aminoestrone-3-methyl ether radiotracer was synthesized to study its inflammatory binding specificity as a novel selective radiopharmaceutical for inflammation imaging. In-vivo biodistribution study of ^{99m}Tc–2-amino estrone-3-methyl ether complex in both bacterial infection and sterile inflammation showed high and rapid accumulation of ^{99m}Tc–2-aminoestrone-3-methyl ether complex at the site of sterile inflammation compared to bacterial infection sites (target-to-non target ratio equal to 4.12 ± 0.02). This high biological accumulation in inflamed cells suggests that ^{99m}Tc–2-aminoestrone-3-methyl ether complex may be suitable as a potential selective radiotracer able to image inflammatory sites.

Keywords Estrone · Technetium-99m · Inflammation · Imaging

Introduction

Inflammation describes a systemic pathological state associated with several disease processes, including coagulation, neovascularization, ischemia and hypoxia, as occurring in many chronic diseases like cancers [1–3], systemic lupus erythematosus [4–6], rheumatoid arthritis [7], diabetes [8, 9] and atherosclerosis [10]. Detection of the inflamed endothelium via imaging analysis or guide the drug to target lesions is therefore important for early diagnosis and treatment of vascular inflammatory diseases. Different imaging techniques show different diagnostic accuracy. Thus, the diagnosis of inflammatory processes often relies on the detection of anatomical/structural changes of the affected organ depending on the nature of the inflammation under investigation. One goal of different imaging techniques is to integrate the diagnostic information combining anatomical with functional data in order to describe and characterize the site, and activity of the disease under investigation. The anatomical description and the spatial relationships of a lesion is well investigated by using radiological imaging procedures such as X-ray, ultrasonography (US), computed tomography (CT), and magnetic resonance imaging (MRI) whereas nuclear medicine provides ideal imaging techniques for the study of functional and histological changes in inflammatory processes [11–15]. The increasing knowledge on the pathogenesis of inflammatory processes lead to the development of radiolabeled receptor ligands, such as peptides, antibiotics, liposomes etc., able to bind in-vivo to specific receptors, specifically expressed or over expressed on cells or tissues of the inflamed organ. These compounds bind to their specific receptors with high affinity (in a nano molar range) [16–18]. Among the receptor-specific radiopharmaceuticals, some radiotracers allow to distinguish among acute and chronic infection/inflammation, because their receptors are expressed on different cells. Unfortunately, most of these compounds are not able to discriminate between sterile inflammation and infection.

On the other hand, estrogens participate in several biological processes through different molecular mechanisms.

M. S. Al Mutairi · N. G. Haress · W. A. Zaghary (✉)
Department of Pharmaceutical Chemistry, College of Pharmacy, King Saud University, Riyadh 11451, Saudi Arabia
e-mail: wzaghary@yahoo.com

M. A. Motaleb
Labeled Compound Department, Hot Labs Center, Atomic Energy Authority, Cairo 13759, Egypt

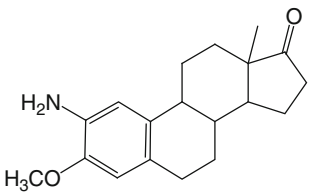

Fig. 1 2-Aminoestrone-3-methyl ether

Their final actions consist of a combination of both direct and indirect effects on different organ and tissues. In general, acute loss of estrogens increases the levels of reactive oxygen species and activates nuclear factor-kB and pro-inflammatory cytokine production, indicating their predominant anti-inflammatory properties. Furthermore, pro-inflammatory cytokine expression has been shown to be attenuated by estrogen replacement [19]. Other researchers reported that estrogens, estrogen receptor-α (ERα), and estrogen receptor-β (ERβ) regulate adipose tissue distribution, inflammation, fibrosis, and glucose homeostasis [20, 21]. In addition to that, certain study revealed that estrogens and androgens are capable of offering disease protection during experimental autoimmune encephalomyelitis [22]. Also, ^{99m}Tc-labeled 17α-triazolylandrost-4-ene-3-one complex was prepared and tested for antiprostatic cancer activity [23]. Recently ^{99m}Tc (I)-estradiol-pyridin-2-yl hydrazine derivative was developed for the diagnostic imaging of breast and endometrial cancers [24]. Estrogens may have pro- and anti-inflammatory properties depending on the situation and the involved tissue [25–32]. The aim of nuclear medicine in the field of inflammation/infection is to develop non-invasive tools for the in-vivo detection of specific cells and tissues; the sensitivity of these techniques usually allow to detect early pathophysiological changes, before the development of anatomical changes, detectable by conventional radiographic techniques and before the clinical onset of the disease. This study was aimed at assessing the performance of labeling yield 2-aminoestrone-3-methyl ether (2-NH_2E1MeO, Fig. 1) with technetium-99m efficiently and studying the factors affecting the labeling yield in details. Moreover, the study of the biodistribution of ^{99m}Tc–2-aminoestrone-3-methyl ether, and evaluate it as a potential radiotracer used for in-vivo imaging of inflammation.

Experimental

General

Melting point (°C, uncorrected) was determined in open glass capillaries using a Barnstead 9001 Electrothermal melting point apparatus. Ultraviolet (UV) spectra were recorded for MeOH solutions (1 mg) on Ultrospec-2100 Pro UV visible spectrophotometer. Infrared (IR) spectra were recorded for potassium bromide discs, ν (cm^{-1}) on Perkin Elmer 1430 spectrophotometer. ^{1}H NMR and ^{13}C NMR spectra were determined on Ultrashield Bruker Biospin (300 MHz) Spectrometers. Chemical shifts are expressed as δ values (ppm) using tetramethylsilane (TMS) as internal reference. Mass spectra (MS) were obtained on GS/MS QP 1000 EX Shimadzu Spectrometer. All chemicals were of analytical grade and used directly without further purification. Deionized water was used in all experiments for the preparation of all solutions. Technetium-99 m was eluted as $^{99m}TcO_4^-$ from ^{99}Mo/^{99m}Tc generator, Elutec Brussels, Belgium. A NaI (Tl) γ-ray scintillation counter (Scaler Ratemeter SR7, Nuclear Enterprises, Edinburgh, England) was used for radioactivity measurements. HPLC equipment was Hitachi model, Alphabond C18 125A 10U column with ID 3.9 and length 300 mm, Tokyo, Japan. Follow up of the reaction and checking the homogeneity of the compound was made by ascending thin layer chromatography (TLC) run on pre-coated (0.25 mm) (GF 254) silica gel plates. The ratio of the solvent systems used as eluents were volume to volume. Routinely used developing solvents systems were: C_6H_6:EtOAc:$CHCl_3$ (5:1:5). Visualization of the spots was performed by exposure to UV lamp at 254 nm. Silica gel (60-230 mesh E. Merck), activated by heating at 110 °C for 1 h and was employed for column chromatography separations. Silica gel 60 GF_{254} for TLC was used for coating 20 × 20 cm glass plates for preparative TLC. All statistical analyses were done using Graph Pad Prism version 6.0 software. Statistical analysis was conducted using one-way ANOVA followed by multiple Tukey–Kranes post hoc test @ $P < 0.05$ considered for statistical significance.

Chemistry

Synthesis of 2-aminoestrone-3-methyl ether (2-NH_2E1MeO) (1) [33, 34]

Sodium dithionite (5 g, 0.027 mol) was added to a hot solution of 2-nitroestrone-3-methyl ether. (1.5 g, 4.5 mmol) in acetone (200 ml) containing 0.5 N aqueous NaOH solution (50 ml) and the mixture was heated under reflux for 35 min. Further amounts of sodium dithionite (4 g, 0.021 mol) and 0.5 N NaOH solution (50 ml) were added and reflux continued for further 40 min. After cooling, H_2O (150 ml) was added and almost all acetone removed under reduced pressure. The milky suspension so produced was left in an ice-bath for 2 h to deposit the product which was filtered, washed with H_2O and dried to give 750 mg (55 %) of 2-aminoestrone-3-methyl ether.

Crystallization from MeOH yielded colourless needles melting at 174–75 °C. Reported mp = 164–65 °C (172), 172.5–174.5 °C (rhombs) and 160.5–162.5, 170–73 and 174–75 °C (needles). IR (KBr) υ (cm^{-1}): 3451 and 3342 (NH free and associated), 1725 (C=O), 1625 (C=C aromatic), 1224 and 1050 (ν_s C–O–C) and at 1513 (δ NH). ^{1}H NMR (DMSO-d_6) δ ppm (300 MHz): 0.80 (s, 3H, C-18–CH_3), 1.33–2.51 (hump, br, 15 H, rings B, C, and D protons), 3.73 (s, 3H, OCH_3), 4.29 (s, 2H, NH_2), 6.54 (s, 1H, C-1–H), and 6.640 (s, 1H, C-4–H). ^{13}C NMR (DMSO-d_6) δ ppm (300 MHz): 14.0 (C-18–CH_3), 21.7 (OCH_3), 24.7 (C-15), 26.2 (C-11), 27.0 (C-7), 32.1 (C-6), 35.9 (C-12), 37.8 (C-16), 44.3 (C-8), 47.8 (C-9), 49.8 (C-13), 55.8 (C-14), 107.1 (C-1), 118.9 (C-4), 119.7 (C-5), 131.2 (C-2), 132.7 (C-10), 143.9 (C-3), 220.3 (C-17). MS *m/z* (% relative abundance): M+ for $C_{19}H_{25}NO_2$ 299 (100), 284 (15), 174 (11), 160 (11), 136 (11), 130 (16), 122 (33), 115 (15), 97 (8), 93 (10), 91 (13), 79 (11), 77 (14), 57 (13), 55 (45), 53 (17), 44 (11), 43 (31), 42 (20), 41 (59).

Preparation of ^{99m}Tc–2-NH_2E1MeO complex

Labeling procedure

The direct labeling technique was used to prepare ^{99m}Tc–2-NH_2E1MeO complex. Accurately weighed 60 mg 2-aminoestrone-3-methyl ether was dissolved in N_2-purged dimethyl sulfoxide and transferred to an evacuated penicillin vial. N_2-purged stannous chloride aqueous solution (containing exactly 1 mg $SnCl_2{\cdot}2H_2O$) was added and the pH of the mixture was adjusted to 1. Then the volume of the mixture was adjusted to 1 ml by N_2-purged distilled water. One ml of freshly eluted $^{99m}TcO_4^-$ (400 MBq) from ^{99}Mo/^{99m}Tc generator was added to the above reaction mixture. The reaction mixture was then vigorously shaken and allowed to react at 80 °C for sufficient time (30 min) to complete the reaction.

Analysis of ^{99m}Tc–2-aminoestrone-3-methyl ether complex

The labeling yield of ^{99m}Tc–2-NH_2E1MeO complex was assessed by using ascending paper chromatographic technique and HPLC. The radiochemical purity and purification of ^{99m}Tc–2-aminoestrone-3-methyl ether complex was performed by thin layer chromatographic method using strips of silica gel impregnated glass fibre sheets (ITLC-SG). Free $^{99m}TcO_4^-$ in the preparation was determined using acetone as the mobile phase. Reduced hydrolyzed technetium was determined using ethanol:water:ammonium hydroxide mixture (2:5:1) as the mobile phase. ^{99m}Tc–ligand complex was further confirmed by a Shimadzu HPLC system, which consists of pumps LC-9A, UV spectrophotometric detector operated at a 220 nm (SPD-6A), and rheodyne injection valve. Chromatographic analysis of ^{99m}Tc–2-NH_2E1MeO complex was performed by injection of 10 μL of the reaction mixture at the optimum conditions into a reversed-phase column, (Waters, Symmetry C18; 5 μm, 4.6 mm × 150 mm) preceded by a guard column (Waters, Symmetry C18; 5 μm) and eluted with mobile phase consisting of acetonitrile and 0.01 M potassium dihydrogen phosphate/diethylamine (60:40:0.2 v/v) [35]. The mobile phase was filtered and degassed prior to use and the flow rate was 0.5 ml/min. The fractions of 0.5 ml (up to 20) were collected separately using a fraction collector and counted in a well-type NaI (Tl) detector connected to a single-channel analyzer.

Biodistribution study

The study was approved by the animal ethics committee and was in accordance with the guidelines set out by the Egyptian Atomic Energy Authority.

Induction of infectious foci

A single clinical isolation of *Staphylococcus aureus* from biological samples was used to produce focal infection. Individual colonies were diluted in order to obtain turbid suspension. Groups of three mice were intramuscularly injected with 200 μl of the suspension in the left lateral thigh muscle. Twenty-four hours required to get gross swelling in the infected thigh.

Induction of non-infected inflammation

Sterile inflammation was induced by injecting 200 μl of turpentine oil sterilized by autoclaving at 121 °C for 20 min, intramuscularly in the left lateral thigh muscle of the mice. Two days later, swelling appeared. Differences in the data were evaluated with the Student *t* test. Results for *P* using the 2-tailed test are reported and all results are given as mean ± SEM. The level of significance was set at $P < 0.05$.

Bio-distribution studies in animals

The biodistribution of the ^{99m}Tc–2-NH_2E1MeO complex was evaluated in male Sprague–Dawley rats (body mass 130–160 g). To induce the inflammation, approximately 105–106 colony forming units of *S. aureus* suspended in 0.2 ml of saline was administrated into the left thigh. For quantitative determination of organ distribution, five rats were used for each experiment and 0.1 ml of about 18 MBq of ^{99m}Tc–2-NH2E1MeO complex solution was

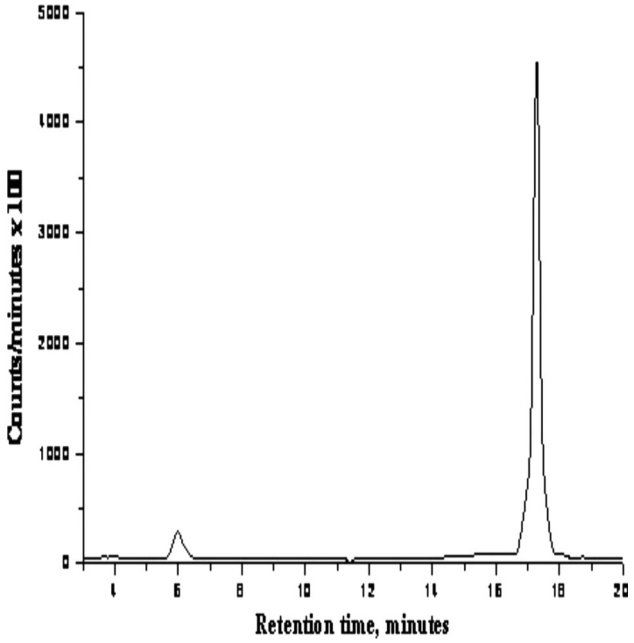

Fig. 2 HPLC radiochromatogram of ^{99m}Tc–2-NH_2E1MeO complex

injected into the tail vein of rats after 24 h of bacterial induction. Then, the rats were killed and blood was obtained by cardiac puncture. Samples of fresh blood, bone, and muscle were collected in pre-weighed vials and counted. The different organs were removed, counted, and compared to a standard solution of the labeled compound. The average percent values of the administrated dose/organ were calculated. Blood, bone, and muscles were assumed to be 7, 10, and 40 %, respectively, of the total body weight. Corrections were made for background radiation and physical decay during experiment. Both target and non-target thighs were dissected and counted. Target and non-target thigh radioactivity ratio was also determined [36].

Results and discussion

The radiochemical yield of ^{99m}Tc–2-NH_2E1MeO complex was determined by using thin layer chromatography (TLC-SG) as well as HPLC. Acetone was used with TLC-SG strip to calculate the percentage of free $^{99m}TcO_4^-$ which moved with the solvent front ($R_f = 1.0$) leaving ^{99m}Tc–2-NH_2E1MeO complex and colloid at the origin. Ethanol:water:ammonium hydroxide mixture (2:5:1) was used to check the amount of reduced hydrolyzed technetium (colloid) which remained at the origin ($R_f = 0$) while $^{99m}TcO_4^-$ and ^{99m}Tc–2-NH_2E1MeO migrated with the solvent front ($R_f = 1$). The radiochemical purity was determined by subtracting the sum of the percent of colloid

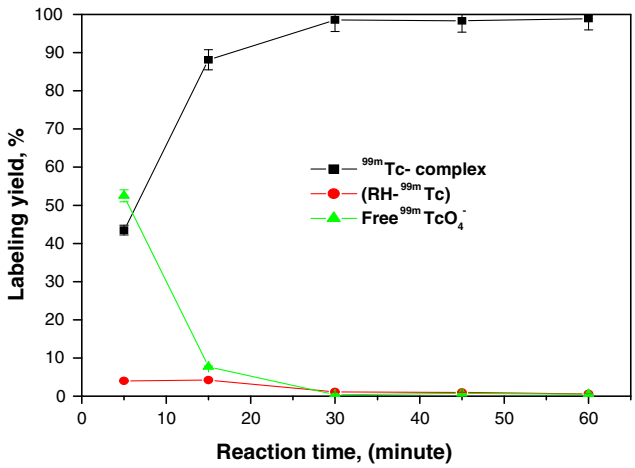

Fig. 3 Effect of the reaction time on the radiochemical yield of ^{99m}Tc–2-NH_2E1MeO complex

and free pertechnetate from 100 %. The radiochemical yield is the mean value of three experiments.

In case of HPLC, an HPLC radiochromatogram is presented in Fig. 2. It exhibited two peaks, one at fraction number 5.8 corresponding to $^{99m}TcO_4^-$, while the second peak was collected at fraction number 17.9 corresponding to ^{99m}Tc–2-NH_2E1MeO complex, which was found to coincide with the UV signal. Nearly, 97 % of the injected activity in the HPLC was recovered as collected activity.

Factors affecting the labeling yield of ^{99m}Tc–2-NH_2E1MeO complex

Various factors affecting the labeling yield of ^{99m}Tc–ligand complex were studied using the ascending paper chromatography analysis. These factors were ligand content, $SnCl_2{\cdot}2H_2O$ content, pH, reaction time, and in-vitro stability.

Effect of reaction time

The radiochemical yield of ^{99m}Tc–2-NH_2E1MeO complex was studied at different reaction times (5–60 min) in the presence of stannous chloride dihydrate and pH 7 as shown in Fig. 3. It is clear that the labeling yield increased from 43.5 to 98.5 % by increasing the reaction time from 5 to 30 min. The radiochemical yield reaches the saturation value and is not affected by increasing the reaction time above 30 min.

Effect of reaction temperature

The effect of reaction temperature on the percent labeling yield of ^{99m}Tc–2-NH_2E1MeO complex was investigated at

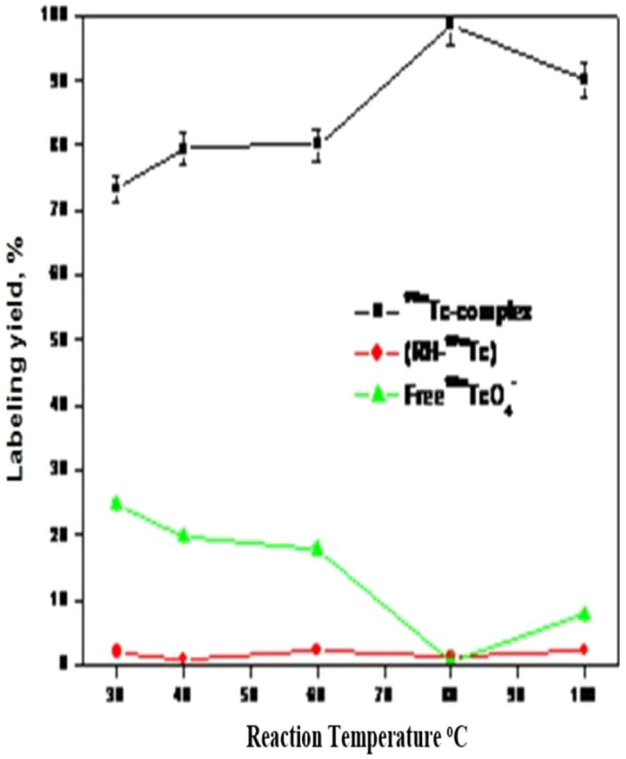

Fig. 4 Effect of temperature on the percent labeling yield of ^{99m}Tc–2-NH_2E1MeO complex

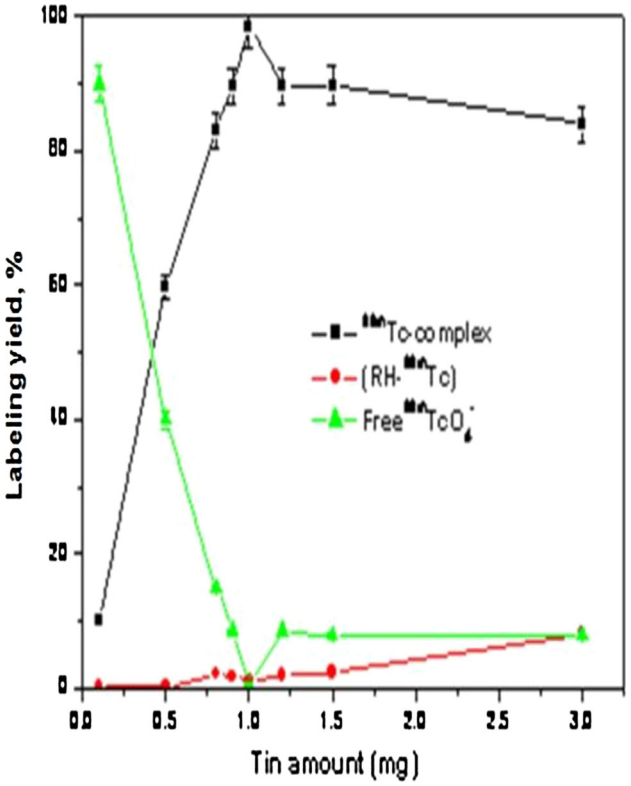

Fig. 5 Effect of Sn(II) content on the percent labeling yield of ^{99m}Tc–2-NH_2E1MeO complex

30, 40, 60, 80 and 100 °C. It is clear from the obtained data that the labeling yield was increased with increasing temperature up to 80 °C where a highest labeling yield was achieved. It should be pointed out that 30 min reaction time was enough to achieve a high labeling yield of ^{99m}Tc–2-aminoestrone-3-methyl complex at 80 °C as shown in Fig. 4.

Effect of Sn(II) content

For labeling with technetium-99m, it is necessary to reduce Tc^{7+} to its more reactive lower oxidation states. Similar to $^{99m}TcO_4^-$, the reduction of $^{99m}TcO_4^-$ is generally accomplished by the addition of $SnCl_2$ in acidic medium. The effect of Sn(II) content on the labeling of 2-aminoestrone-3-methyl ether was studied in the range of 0.1–3 mg. It is clearly obvious from Fig. 5 that using too little stannous chloride resulted in incomplete reduction of $^{99m}TcO_4^-$, which led to the presence of much free $^{99m}TcO_4^-$ and a poor labeling yield. However, as the concentration of stannous chloride was increased, the labeling yield also increased. The optimum amount of Sn(II) content was found to be 1 mg. If too much Sn(II) is used, the amount of ^{99m}Tc-Sn-colloid and/or reduced hydrolysed ^{99m}Tc increased, thus decreasing the labeling yield.

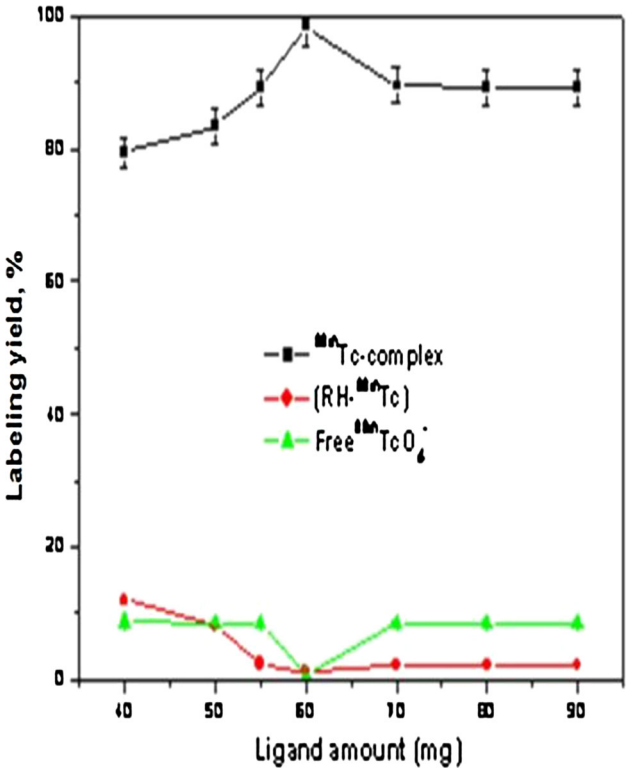

Fig. 6 Effect of 2-aminoestrone-3-methyl ether content on the percent labeling yield of ^{99m}Tc–2-NH_2E1MeO complex

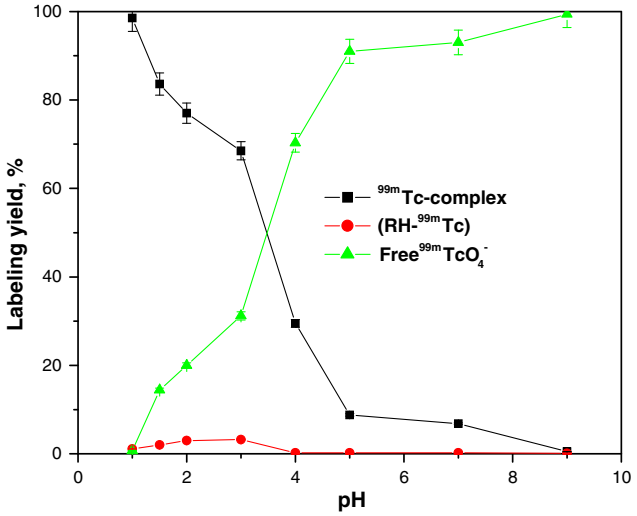

Fig. 7 Effect of the pH value on the percent labeling yield of ^{99m}Tc–2-NH_2E1MeO complex

Effect of ligand content

The influence of the ligand content on the labeling yield of ^{99m}Tc–2-aminoestrone-3-methyl ether complex was investigated in the range of 40–90 mg and the results are presented in Fig. 6. It is clearly obvious from this figure that at low quantity of the ligand the labeling yield was low and this may be attributed to insufficient amount of the ligand required to bind all the reduced Tc, while a white precipitate was formed. The labeling yield increased by increasing the amount of ligand up to 60 mg, above this amount the labeling yield remained unchanged and the highest obtained labeling yield was 98.5 ± 3.4 %.

Effect of pH of the reaction mixture

The effect of pH of the reaction mixture on the labeling yield of ^{99m}Tc–2-NH_2E1MeO complex in the pH range 0.7–9.0

Table 1 Biodistribution of ^{99m}Tc–2-NH_2E1MeO complex in turpentine inflammated mice

Organs and body fluids	Percent I.D./gram organ			
	Time post injection (min)			
	15	30	60	120
Blood	9.54 ± 0.04	4.27 ± 0.12	1.23 ± 0.02	0.97 ± 0.07
Control muscle	0.27 ± 0.01	0.28 ± 0.01	0.24 ± 0.00	0.20 ± 0.02
Infected muscle	0.38 ± 0.02	0.65 ± 0.02	0.99 ± 0.01	0.48 ± 0.05
Liver	19.40 ± 1.05	22.06 ± 0.95	33.57 ± 1.15	35.31 ± 1.16
Intestine	6.54 ± 0.50	9.18 ± 0.25	13.46 ± 0.30	14.84 ± 0.39
Kidney	2.32 ± 0.14	3.41 ± 0.20	4.66 ± 0.19	5.26 ± 0.30
Lung	2.47 ± 0.01	1.03 ± 0.11	0.96 ± 0.05	1.27 ± 0.12
Stomach	1.60 ± 0.15	3.04 ± 0.29	4.45 ± 0.03	10.27 ± 0.09
Heart	0.48 ± 0.05	0.41 ± 0.03	0.16 ± 0.01	0.48 ± 0.02
Spleen	3.10 ± 0.33	2.33 ± 0.32	1.32 ± 0.09	1.49 ± 0.12
T/NT	1.41 ± 0.01	2.32 ± 0.03	4.12 ± 0.02	2.40 ± 0.07

Values represent mean ± SEM ($n = 5$)

Significantly different from previous value of each organ using unpaired Student's t test ($P < 0.05$)

Table 2 Biodistribution of ^{99m}Tc–2-NH_2E1MeO complex in bacteria inflammated mice

Organs and body fluids	Percent I.D./gram organ			
	Time post injection (min)			
	15	30	60	120
Blood	7.94 ± 0.03	4.8 ± 0.11	0.92 ± 0.01	0.90 ± 0.02
Control muscle	0.54 ± 0.10	0.5 ± 0.01	0.45 ± 0.02	0.45 ± 0.10
Infected muscle	1.0 ± 0.20	0.72 ± 0.06	0.6 ± 0.02	0.50 ± 0.60
Liver	17.20 ± 1.08	21.09 ± 0.65	31.29 ± 1.35	32.21 ± 1.21
Intestine	7.55 ± 0.30	9.16 ± 0.21	15.26 ± 0.20	17.71 ± 0.19
Kidney	4.5 ± 0.10	5.20 ± 0.10	12.2 ± 1.10	10.2 ± 0.30
Lung	3.09 ± 0.91	2.86 ± 0.41	2.87 ± 0.12	2.47 ± 0.22
Stomach	0.17 ± 0.09	3.69 ± 0.29	4.58 ± 0.30	11.73 ± 0.66
Heart	0.25 ± 0.00	0.52 ± 0.15	0.30 ± 0.05	1.60 ± 0.21
Spleen	0.50 ± 0.02	0.90 ± 0.10	2.20 ± 0.10	1.30 ± 0.03
T/NT	1.85 ± 0.05	1.44 ± 0.07	1.33 ± 0.01	1.11 ± 0.0

Values represent mean ± SEM ($n = 5$)

Significantly different from previous value of each organ using unpaired Student's t test ($P < 0.05$)

was investigated. Figure 7 shows that a higher percent labeling yield (98.5 ± 3.4 %) was obtained at pH 1. The percent labeling yield was gradually decreased till pH 3. A sharp decrease of the labeling yield was obtained above pH 3.

Biodistribution in inflamed mice

The uptake of the ^{99m}Tc–2-NH_2E1MeO complex in important body organs and fluids of the animals injected with turpentine oil and bacteria was given in Tables 1 and 2, respectively. ^{99m}Tc–2-NH_2E1MeO complex was removed from the circulation mainly through the hepatobiliary pathway (approximately 50 % injected dose after 2 h after injection of the tracer). Rats with infectious lesions injected with ^{99m}Tc–2-NH_2E1MeO complex showed a maximum mean abscess-to-muscle (target-to-non target, T/NT) ratio equal to 1.85 ± 0.05 at 15 min. The accumulation of activity at the site of infection was maximized at 15 min after intravenous injection then slightly decreased with time until T/NT equal to 1.11 at 120 min post injection. On the other hand, mice with inflammation injected with ^{99m}Tc–2-NH_2E1MeO complex showed a mean abscess-to-muscle (target-to-non target, T/NT) ratio equal to 4.12 ± 0.02, after 60 min post injection. ^{99m}Tc–2-NH_2E1MeO complex showed higher T/NT in the sterile inflamed muscle (turpentine) at 60 min intervals than that of infected muscle (Bacteria). So, ^{99m}Tc–2-aminoestrone-3-methyl ether complex can differentiate bacterial infection from sterile inflammation. As a result, ^{99m}Tc–2-aminoestrone-3-methyl ether complex showed higher uptake in inflamed tissue and can be used as a possible inflammatory imaging agent.

Conclusion

2-Aminoestrone-3-methyl ether was labeled with ^{99m}Tc by direct labeling method with a high labeling yield. A comparative biodistribution study of ^{99m}Tc–2-aminoestrone-3-methyl complex in both bacterial infection and sterile inflammation demonstrated high and rapid accumulation of ^{99m}Tc–2-NH_2E1MeO complex at the site of sterile inflammation compared to bacterial infection sites. The results also indicated also that the new ^{99m}Tc–2-NH_2E1MeO complex is rapidly cleared from the body through the hepatobiliary pathway.

Acknowledgments This research project was supported by a grant from the "Research Center of Female Scientific and Medical Colleges", Deanship of Scientific Research, King Saud University.

References

1. Yang M, Liu C, Niu M, Hu Y, Guo M, Zhang J, Luo Y, Yuan W, Yang M, Yun M, Guo L, Yan J, Liu D, Liu J, Jiang Y (2014) Phage-display library biopanning and bioinformatic analysis yielded a high-affinity peptide to inflamed vascular endothelium both in-vitro and in-vivo. J Controlled Release 174:72–80
2. Zehnder P, Jenni W, Aeschlimann AG (1998) Systemic vasculitis and solid tumors (epitheliomas). Rev Rhum Engl Ed 65:442
3. Fain O (2002) Vasculitis and cancers. Rev Med Intern Found Soc Natl Fr Med Intern 23(Suppl. 5):551–553
4. Lee CK, Lee TH, Lee SH, Chung IK, Park SH, Kim HS, Kim SJ (2010) GI vasculitis associated with systemic lupus erythematosus. Gastrointest Endosc 72:618–619
5. Hervier B, Hamidou M, Haroche J, Durant C, Mathian A, Amoura Z (2012) Systemic lupus erythematosus associated with ANCA-associated vasculitis: an overlapping syndrome? Rheumatol Int 32:3285–3290
6. Butendieck RR, Parikh K, Stewart M, Davidge-Pitts C, Abril A (2012) Systemic lupus erythematosus-associated retinal vasculitis. J Rheumatol 39:1095–1096
7. Radic M, Kaliterna DM, Radic J (2013) Overview of vasculitis and vasculopathy in rheumatoid arthritis—something to think about. Clin Rheumatol 32:937–942
8. Hartge MM, Unger T, Kintscher U (2007) The endothelium and vascular inflammation in diabetes. Diabetes Vasc Dis Res 4:84–88
9. Onat D, Brillon D, Colombo PC, Schmidt AM (2011) Human vascular endothelial cells: a model system for studying vascular inflammation in diabetes and atherosclerosis. Curr Diabetes Rep 11:193–202
10. Schwartz EA, Reaven PD (2012) Lipolysis of triglyceride-rich lipoproteins, vascular inflammation, and atherosclerosis. Biochim Biophys Acta 1821:858–866
11. Beltram J (1995) MR imaging of soft tissue infection. Magn Reson Imaging Clin N Am 3:743–751
12. Vazquez E, Enriquez G, Castellote A, Lucaya J, Creixell S, Aso C, Regas J (1995) US, CT, and MR imaging of neck lesions in children. Radiographics 15:105–122
13. Welling MM, Paulusma-Annema A, Balter HS, Pauwels EK, Nibbering PH (2000) Technetium-99m labelled antimicrobial peptides discriminate between bacterial infections and sterile inflammations. Eur J Nucl Med 27:292–301
14. Corstens FHM, Van der Meer JWM (1999) Nuclear Medicine's role in infection and inflammation. Lancet 354:760–765
15. Chianelli M, Mather SJ, Martin –Comin J, Signore A (1997) Radiopharmaceutical for the study of inflammatory processes: a review. Nucl Med Comm 18:437–455
16. Okarvi SM (1999) Recent developments in ^{99m}Tc-labelled peptide-based radiopharmaceuticals an overview. Nucl Med Commun 20:1093–1112
17. Boerman OC, Oyen WJG, Corstens FHM (2000) Radio-labeled receptor binding peptides: a new class of radiopharmaceuticals. Semin Nucl Med 30:195–208
18. Signore A, Annovazzi A, Chianelli M, Corsetti F, Van De Wiele C, Watherhouse RN, Scopinaro F (2001) Peptide radiopharmaceuticals for diagnosis and therapy. Eur J Nucl Med 28:1555–1565
19. Martín-Millán M, Castaneda S (2013) Estrogens, osteoarthritis and inflammation. Joint Bone Spine 80:368–373
20. Davis KE, Neinast MD, Sun K, Skiles WM, Bills JD, Zehr JA, Zeve D, Hahner LD, Cox DW, Gent LM, Xu Y, Wang ZV, Khan SA, Clegg DJ (2013) The sexually dimorphic role of adipose and adipocyte estrogen receptors in modulating adipose tissue expansion, inflammation, and fibrosis. Mol Metab 2:227–242

21. Holm A, Andersson KE, Nordström I, Hellstrand P, Nilsson B (2010) Down-regulation of endothelial cell estrogen receptor expression by the inflammation promoter LPS. Mol Cell Endocrinol 319:8–13
22. Spence RD, Voskuhl RR (2012) Neuroprotective effects of estrogens and androgens in CNS inflammation and neurodegeneration. Front Neuroendocrinol 33:105–115
23. Dhyani MV, Satpati D, Korde A, Banerjee S (2011) Synthesis and preliminary bioevaluation of $^{99m}Tc(CO)_3$-17α-triazolylandrost-4-ene-3-one derivative prepared via click chemistry route. Cancer Biotherapy Radiopharm 26:539–545
24. Nayak TK, Hathaway HJ, Ramesh C, Arterburn JB, Dai D, Sklar LA, Norenberg JP, Prossnitz ER (2008) Preclinical development of a neutral, estrogen receptor–targeted, tridentate $^{99m}Tc(I)$-estradiol-pyridin-2-yl hydrazine derivative for imaging of breast and endometrial cancers. J Nucl Med 49:978–986
25. Jiang X, Shapiro DJ (2014) The immune system and inflammation in breast cancer. Mol Cell Endocrinol 382:673–682
26. Edgar AR, Judith PY, Elisa DSM, Rafael CR (2013) Glucocorticoids and estrogens modulate the NF-kB pathway differently in the micro- and microvasculature. Med Hypotheses 81:1078–1082
27. Gosselin D, Rivest S (2011) Estrogen receptor transrepresses brain inflammation. Cell 145:495–497
28. Kovats S (2012) Estrogen receptors regulate an inflammatory pathway of dendritic cell differentiation: mechanisms and implications for immunity. Horm Behav 62:254–262
29. Saint-Criq V, Rapetti-Mauss R, Yusef YR, Harvey BJ (2012) Estrogen regulation of epithelial ion transport: implications in health and disease. Steroids 77:918–923
30. Miller VM, Jayachandran M, Hashimoto K, Heit JA, Owen WG (2008) Estrogen, inflammation, and platelet phenotype. Gend Med 5:91–102
31. Chinenov Y, Gupte R, Rogatsky I (2013) Nuclear receptors in inflammation control: repression by GR and beyond. Mol Cell Endocrinol 380:55–64
32. Fan GW, Gao XM, Wang H, Zhu Y, Zhang J, Hu LM, Su YF, Kang LY, Zhang BL (2009) The anti-inflammatory activities of Tanshinone IIA, an active component of TCM, are mediated by estrogen receptor activation and inhibition of iNOS. J Steroid Biochem Mol Biol 113:275–280
33. Tomsonand AJ, Horwitz JP (1959) Some 2- and 4-substituted estrone 3-methyl ethers. J Org Chem 24:2056–2058
34. Kraychy S (1959) Synthesis of potential metabolites of estradiol. J Am Chem Soc 81:1702–1704
35. Motaleb MA (2007) Preparation of ^{99m}Tc-cefoperazone complex, a novel agent for detecting sites of infection. J Radioanal Nucl Chem 272:167–171
36. Rhodes BA (1974) Consideration in the radiolabeling of albumin. Sem Nucl Med 4:281–293